SCIENTIFIC REPORTS

OPEN

SUBJECT AREAS:
BACTERIOLOGY
GEOCHEMISTRY
FUNCTIONAL CLUSTERING
ECOSYSTEM ECOLOGY

Received
3 December 2012

Accepted
2 April 2013

Published
29 April 2013

Correspondence and requests for materials should be addressed to P.-Y.Q. (boqianpy@ust.hk)

Autotrophic Microbe Metagenomes and Metabolic Pathways Differentiate Adjacent Red Sea Brine Pools

Yong Wang[1], Huiluo Cao[1], Guishan Zhang[1,2], Salim Bougouffa[1], On On Lee[1], Abdulaziz Al-Suwailem[2] & Pei-Yuan Qian[1]

[1]Division of Life Science, Hong Kong University of Science and Technology, Clear Water Bay, Hong Kong, China, [2]King Abdullah University of Science and Technology, Thuwal, The Kingdom of Saudi Arabia.

In the Red Sea, two neighboring deep-sea brine pools, Atlantis II and Discovery, have been studied extensively, and the results have shown that the temperature and concentrations of metal and methane in Atlantis II have increased over the past decades. Therefore, we investigated changes in the microbial community and metabolic pathways. Here, we compared the metagenomes of the two pools to each other and to those of deep-sea water samples. Archaea were generally absent in the Atlantis II metagenome; Bacteria in the metagenome were typically heterotrophic and depended on aromatic compounds and other extracellular organic carbon compounds as indicated by enrichment of the related metabolic pathways. In contrast, autotrophic Archaea capable of CO_2 fixation and methane oxidation were identified in Discovery but not in Atlantis II. Our results suggest that hydrothermal conditions and metal precipitation in the Atlantis II pool have resulted in elimination of the autotrophic community and methanogens.

Along the narrow seafloor of the Red Sea, approximately 25 deep-sea brine pools have been formed by the spreading of the Arabic and African plates[1]. The movement of these plates results in volcanic activity due to breaking of the earth crust. Injection of a geothermal solution into seafloor depression resulted in the development of deep-sea brine pools due to mixing of the hot and metalliferous solution with seawater[2,3]. Two famous brine pools, Atlantis II and Discovery, were discovered in the 1960s and since then, these brine pools have been the focus of geological and geochemical surveys in the Red Sea[4–7]. A number of geological questions have been raised, including questions about the relationship between the two brine pools. Because of their close proximity, it has been suggested that the Atlantis II and Discovery are connected and that brine flows between the two pools[8]. This hypothesis was supported by a parallel change in the anhydrite content in the sediment pore water[9]. Given their proposed historic connection and similar environments, it has been suggested that the pools were inhabited by similar microbial communities that can be exchanged in between.

It is now known that the two brine pools are separated by a sill, which is about 50 m higher than the main brine levels[10] and the two pools have different environmental conditions. The most striking observation was a gradual increase in temperature over the last few decades in the Atlantis II pool from 56 to 68°C[11,12], while the Discovery brine pool has maintained a stable temperature of approximately 44°C[12]. In addition, the methane concentration in the Atlantis II pool is 4-fold higher than that in the Discovery pool[13]. The concentrations of certain metal ions, such as Fe, Mn, Li and Zn, are also much higher in Atlantis II[1]. All of these differences have been attributed to mounting volcanic activity at the bottom of the Atlantis II basin; this activity has supplied the pool with a hydrothermal solution with estimated temperatures and salinities ranging from 195–310°C and 270–370‰, respectively[14]. The Atlantis II brine pool now has three upper convective layers that differ in salinity, temperature, and metal content[7]. In contrast, only one upper layer is evident in the Discovery brine pool[7]. Therefore, since the two pools have different physical and geochemical conditions, it is hypothesized that the microbial inhabitants of these brine pools are also different and have different metabolic activities. The objective of this study was to test this hypothesis.

Our recent metagenomic work has provided a glimpse of the microbes that are present in the pools and focused on the organic maturation process in the Atlantis II pool[15]. However, a comprehensive comparison of the two metagenomes of the microbial communities and their activities has not been conducted. In addition the roles of the microbes in the carbon cycle and metal precipitation in the two brine pools have not been

examined. Analyses of gene profiles and biodiversities within the pools could provide insight into the microbial fitness model in these extreme environments.

In the present study, we analyzed metagenomes from the lower convective layers in the Atlantis II and Discovery brine pools and compared them with two deep-sea water metagenomes. Strong dissimilarities between the brine pool metagenomes were demonstrated with respect to the microbial community and metabolic spectrum. The Atlantis II metagenome was enriched with heterotrophic metal-reducing microbes utilizing aromatic compounds and extracellular organic carbon sources, whereas autotrophic microbes capable of CO_2 fixation and methane oxidation were found in Discovery and functioned as primary producers. Compared with the deep-sea water samples, the brine pool microbes displayed weaknesses in the glyoxylate cycle, oxidative phosphorylation and biosynthesis under anaerobic conditions.

Results

Different microbial communities in the two brine pools. Sampling sites in the Atlantis II and Discovery brine pools are shown in Figure 1[16]. The temperature in the lower convective layer (>2100 m) was 68°C in Atlantis II and 45°C in Discovery. The salinity was 255‰ in both pools. The bacterial cell density in the Atlantis II and Discovery pools was 9,200 and 7,000 cells ml^{-3}, respectively. The brine water samples were pyrosequenced (hereafter referred to as 'ABP' for Atlantis II; 'DBP' for Discovery). The 16S rRNA gene fragments were extracted from the brine metagenomes and two reference deep-sea water metagenomes (CAM: Carmen Basin in the Gulf of California and MED: the Matapan-Vavylov deep in the Mediterranean Sea) to obtain an initial overview of the microbial community based on the RDP classifier[17] (Table 1). In CAM and DBP, Archaea occupied approximately 8% and 47% of their 16S rRNA fragments, respectively. The deep-sea water samples (CAM and MED) were dominated by Gammaproteobacteria as previously reported[18,19], but this dominance was replaced by Betaproteobacteria in ABP (66%) and by Euryarchaeota in DBP (42%). Betaproteobacteria ranked second in DBP (28%). At the genus level, *Cupriavidus* (59% in ABP; 25% in DBP) was the major component of communities in the brine metagenomes (ABP and DBP), and *Alteromonas* (86%) dominated overwhelmingly the MED sample. Additional details about all the other genera have been previously described[15,18,19]. The percentage of known taxa below the phylum level dropped sharply in CAM, and therefore, the dominant genera could not be determined. Approximately 30% of the 16S rRNA gene fragments of CAM could not be determined, consistent with the results of a metatranscriptomic study of a sample from a neighboring site[20]. At the order level, only 25% of the CAM fragments could be recognized; they were particularly difficult to sort into known taxonomies at lower levels, potentially due to the shorter reads obtained for CAM (Table 1).

The taxonomy of a metagenome can also be examined based on gene content. Among the reads, 627,433 and 618,510 complete open

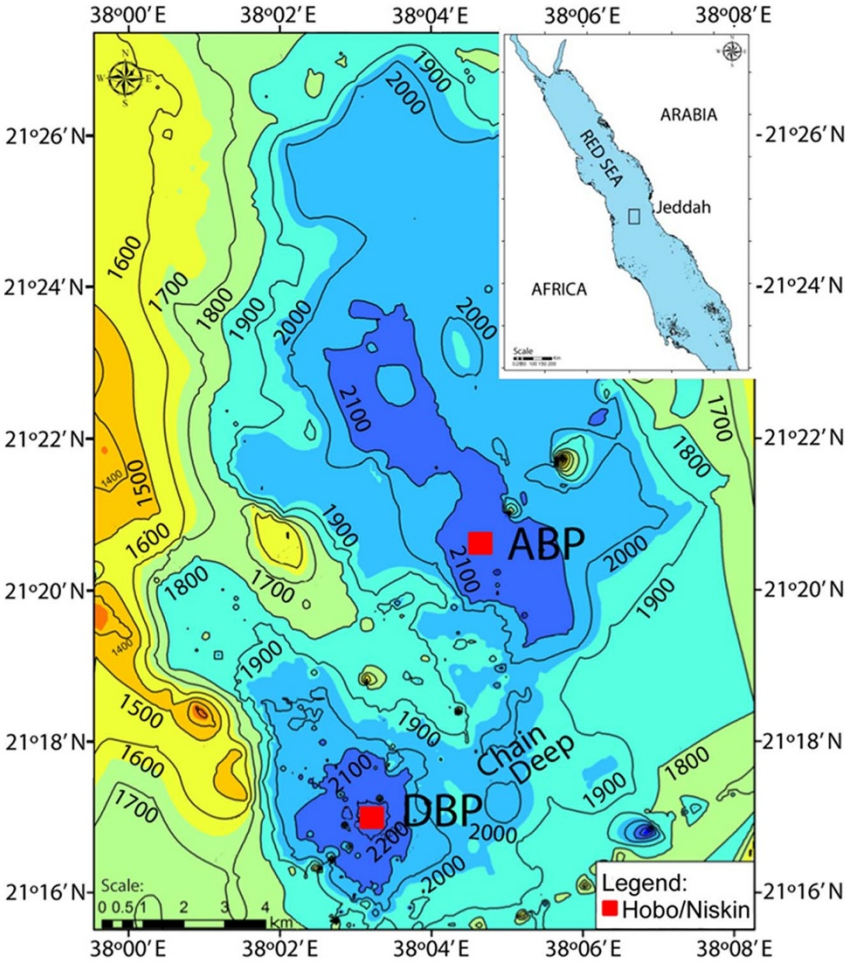

Figure 1 | Geographic map of the sampling sites. Map showing the two sample sites. The Atlantis II (ABP) and Discovery (DBP) brine pools in the Red Sea (inlet), where brine water was collected (at a depth >2100 m) using Niskin bottles. The map was based on bathymetric data obtained using the SIMRAD EK60 echosounder (Kongsberg Maritime AS, Noway) during the KAUST Red Sea Expedition 2010 and contoured using ArcGIS software (ESRI, USA).

Table 1 | Facts of four metagenomes

Sample	No. Reads	Average Length (bp)	Reads for KEGG genes	No.16S rRNAs	%Known phyla	Dominant phylum
ABP	991,323	391	74,475	517	97.7	Betaproteobacteria (66%)
DBP	914,783	410	181,849	321	93	Euryarchaeota (42%)
CAM	462,850	235	80,637	169	65.7	Gammaproteobacteria (29%)
MED	557,800	541	204,750	649	98.3	Gammaproteobacteria (97%)

The metagenomes of ABP from the Atlantis II and DBP from Discovery brine pools were pyrosequenced in this study. CAM from the Gulf of California and MED from Mediterranean Sea are reference deep-sea water metagenomes. The classification results were summarized from the output of the RDP classifier using a confidence cutoff of 50%.

reading frames (cORFs) were collected for ABP and DBP, respectively. Using the BLAST result for the curated cORFs, the taxonomies were summarized for ABP and DBP using MEGAN[21] (Fig. 2). Consistent with the results based on the 16S rRNA gene fragments, Betaproteobacteria (70%) and Euryarchaeota (42%) were the dominant phyla in the corresponding brine microbial communities. Archaea accounted for approximately 50% of the whole community in DBP. In contrast, there were several archaeal reads in ABP. The Euryarchaeota in DBP was mainly composed of Archaeoglobales, Halobacteriales and a group of orders involved in methanogenesis and the anaerobic oxidation of methane (AOM). Regarding the bacterial phyla, DBP had a higher proportion of Firmicutes, Deinococcus-Thermus and Delta/Epsilonproteobacteria compared with ABP. Overall, DBP displayed a higher biodiversity than ABP, as suggested by its two-fold higher Shannon index (2.19 vs. 1.04).

Categories of Clusters of Orthologous Groups (COG) in the four metagenomes. COGs in the reads were sorted into categories. The ABP and DBP brine samples did not consistently display an over or under-representation in the individual categories, as compared with the deep-sea samples (Fig. S1). ABP had the highest percentage of COGs in the following categories: carbohydrate transport and metabolism, lipid metabolism, transcription, intracellular trafficking and secretion, and secondary metabolite biosynthesis, DBP featured the highest level of categories representing DNA replication, recombination and repair among the four metagenomes. This was in accord with the presence of abundant phages in DBP, as indicated by taxonomic assignment of the genes.

Examination of the Kyoto Encyclopedia of Genes and Genomes (KEGG) genes and pathways to show the relationship between samples. Because the results for the COG categories revealed a lack of congruency among the brine or the deep-sea samples, KEGG genes were used to examine differences and similarities among the samples. A Bray-Curtis dissimilarity matrix was calculated using standardized frequencies of the KEGG genes. Subsequently, a relationship based on an agglomerative hierarchical clustering (AHC) was displayed (Fig. 3). The position at which MED and CAM merged was below the primary merging dissimilarity level of 0.52 in AHC, and therefore, they could be grouped together. Although ABP and DBP were obtained from adjacent brine pools, they could not be merged together. Principal coordinates analysis

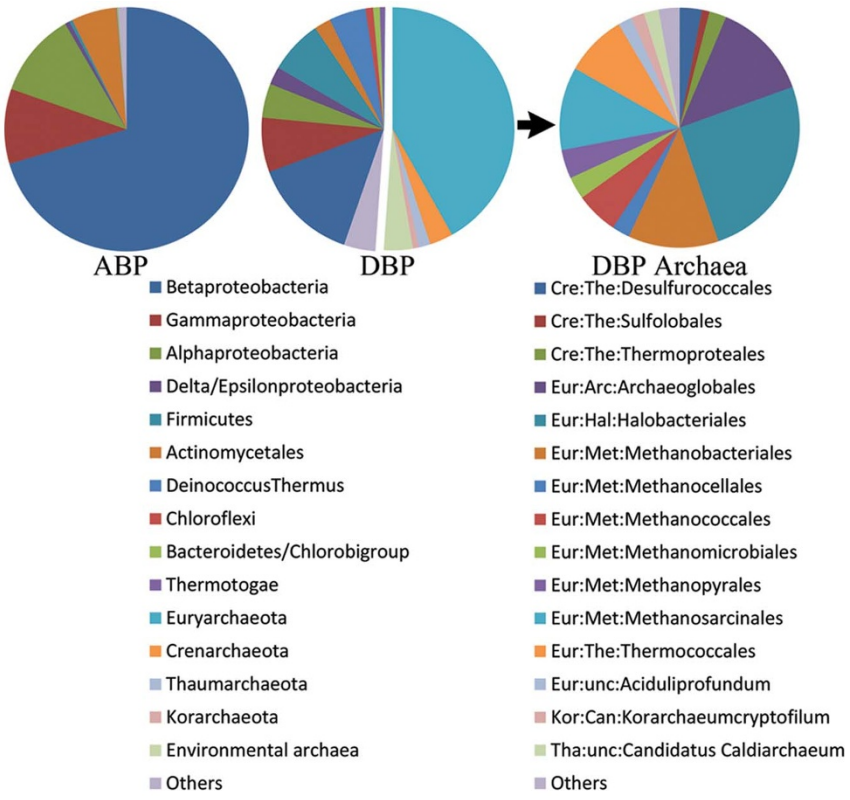

Figure 2 | Taxonomic assignment of ABP and DBP cORFs. Taxonomic assignment was based on the taxa of the ABP and DBP cORFs following a BLAST search against the NCBI protein database. Archaea accounted for approximately 50% of the microbial community in DBP, and they were then classified down to the level of order.

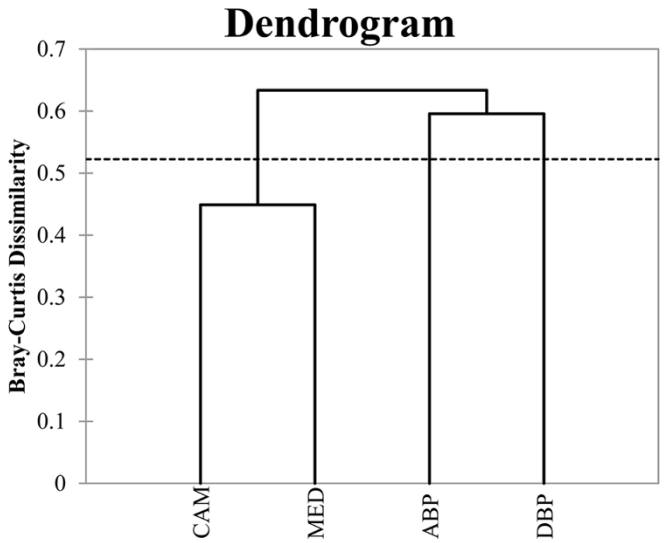

Figure 3 | Agglomerative hierarchical clustering of KEGG genes. The dashed line refers to the minimum dissimilarity level at which the samples were grouped.

(PCoA) was employed to further illustrate the relationship between the samples. In a plot of the principal coordinates F1 and F2, the four samples were widely separated (Fig. 4), suggesting a distant relationship among the samples on a large scale. Despite this finding, close relationships were illustrated in pair-wise plots of other coordinates. ABP and CAM showed a closer relationship in the plot of F1 and F3; DBP and MED were the closest neighboring points in the plot of F2 and F3 (Fig. 4), which indicated that similarities in gene abundance persisted in a small fraction of the genes in DBP and MED. However, the results also indicated that environmental differences might have drastically shifted the microbial communities and their metabolic processes. Thus, we focused next on determining which genes and pathways were responsible for the disparities.

The KEGG genes were clustered based on their relative abundance after normalization according to the z-score. The results from the sample clustering using a complete linkage method were consistent with those obtained for the AHC analysis (Figs. 3 and 5). In the heat map of the gene profiles, sample-specific enriched gene clusters occupied a large part of the region, but commonly enriched clusters were rare, in agreement with the large distance between the samples in the plot of principal coordinates F1 and F2 (Figs. 4 and 5). There were pathways represented by the genes present in five hot regions, areas I to V in Figure 5. A high level of pathway completeness suggested their adaptive importance within a given sampling site. For instance, ABP-specific region I comprised genes affiliated with pathways that participate in the degradation of aromatic compounds and non-aromatic cyclic organic carbon, butanoate metabolism, nitrogen fixation, unsaturated fatty acids synthesis and lipid metabolism. The completeness of these pathways was striking. Together with the findings from the COG category analysis regarding carbohydrate transport and metabolism, the microbes present in ABP were generally heterotrophic bacteria that depended heavily on extracellular aromatic and other organic carbon sources.

Some of the gene clusters specific to DBP in region II were affiliated with CO_2 fixation and methane metabolism, and these pathways displayed a high level of completeness. Sugar utilization in DBP was inferred from the pathway map for starch and sucrose metabolism, in which starch, sucrose, isomaltose, extracellular trehalose, and cellulose were potential sugar sources based on the Enzyme Commission (EC) numbers in the map. Region III for MED contained dozens of genes involved in carotenoid biosynthesis,

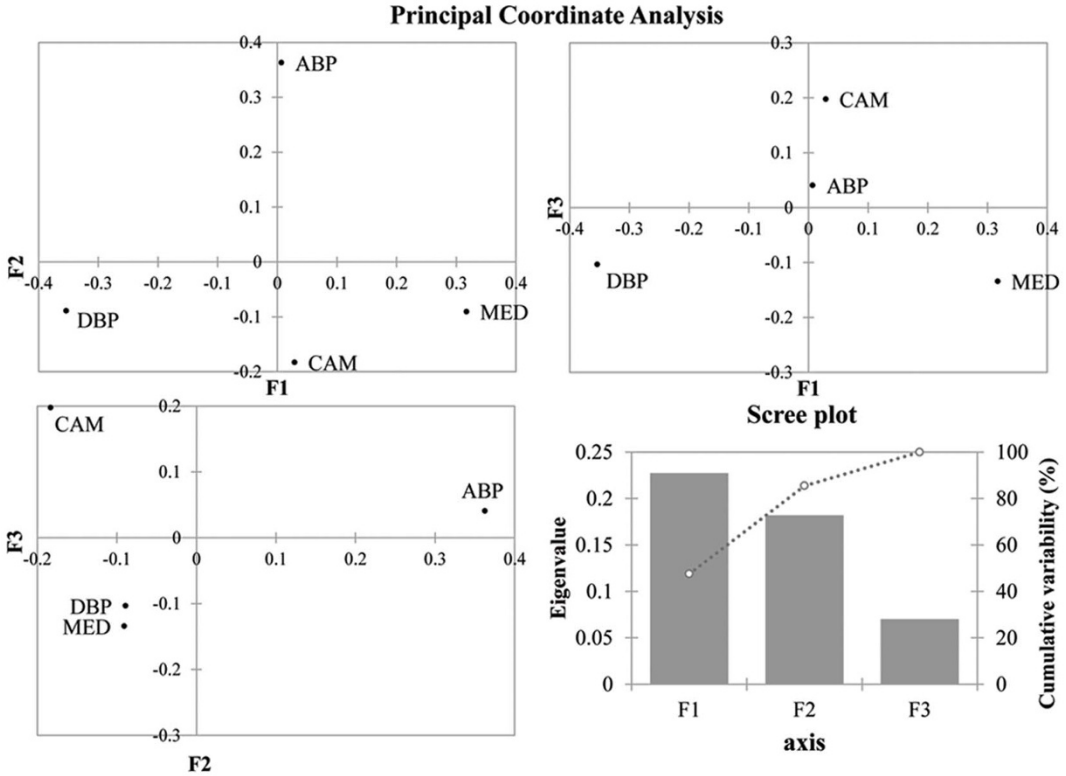

Figure 4 | Principal coordinate analysis results. Principal coordinate analysis and the scree plot revealed three principal coordinates (axes). The three plots were generated using different combinations of the principal coordinates.

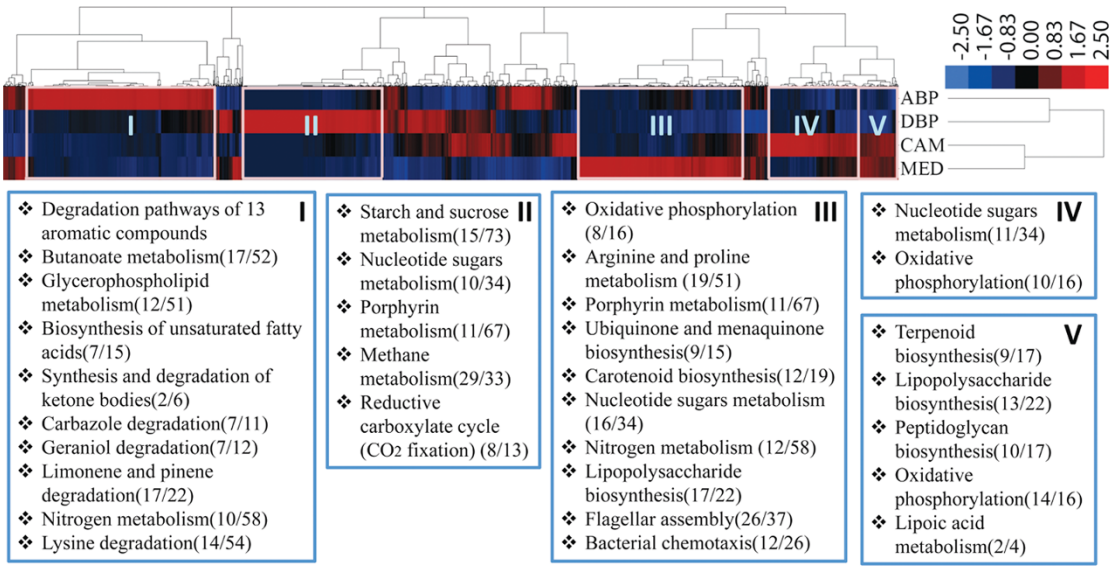

Figure 5 | Sorting of sample-specific enriched gene clusters into pathways. The frequencies of KEGG genes were normalized using the z-score and clustered together with the samples. Genes present in the five regions of the heat map (I-V) were assigned to different KEGG pathways. The same pathways appeared in different regions, but the list of genes (sometimes encoding subunits of an enzyme) was different. The number of identified genes and the total number of enzymes in the pathways are indicated in parentheses.

nitrogen metabolism (denitrification), flagellar assembly and bacterial chemotaxis. Region V comprised genes that were commonly enriched in CAM and MED and showed a high completeness of the terpenoid biosynthesis pathway. For CAM and MED, regions III-V showed a strong representation of oxidative phosphorylation and cell membrane synthesis pathways among the enriched genes. The specific genes involved in oxidative phosphorylation differed among the three regions as discussed below.

Functional modules of the KEGG genes in Figure 5 are summarized in Table S1. Based on the completeness of the modules, metabolic and adaptive activities were demonstrated, particularly those conducted by ATP-binding cassette (ABC) transporters and two-component systems in a metagenome. Many transporter genes involved in the transmembrane transport of various amino acids and sugars were found in region I for ABP. Strikingly, almost all of the gene members in the type IV and VI secretion systems were enriched in ABP. A special assignment of genes into modules for V-type ATP generation (typically the archaeal type), methanogenesis and CO_2 fixation highlighted their importance in DBP. Metal ion pumps of the cobalt/nickel/iron complex and manganese/iron showed fairly complete representation as well. In region III, the presence of cytochrome c oxidase genes in the cbb3 type was associated with a strong pentose phosphate module, which was indicative of a response to the low oxygen concentration in the MED sampling site[19,22]. Genes encoding ABC polysaccharide transporters were also concentrated in this region. In addition, the type II general secretion system was highly represented in MED. For CAM, region IV was characterized by genes specific to pathways that participate in NADH dehydrogenation (complex I in oxidative phosphorylation), pyrimidine nucleotide biosynthesis and dTDP sugar biosynthesis. Region V contained modules capable of heme transport, cytochrome c oxidation-reduction (complex IV in oxidative phosphorylation), F-type ATP generation (complex V in oxidative phosphorylation, bacterial type), C5 isoprenoid biosynthesis, and lipopolysaccharide biosynthesis. These modules allowed us to further dissect the characteristic metabolic processes exemplified by the KEGG pathways in different samples.

CO_2 fixation processes. DBP contained hundreds of reads for the ECs, particularly EC1.2.7.3 (K00174-K00177) and EC1.2.7.1 (K00169-K00172), which are typically involved in autotrophic and anaplerotic CO_2 fixation. The two ECs mediate the reaction of succinyl-CoA + CO_2 → 2-oxoglutarate (part of the reductive citric acid cycle (rTCA)) and catalyze acetyl-CoA + CO_2 → pyruvate (reductive acetyl-CoA reaction; rACA), respectively[23]. Homologs present in the other samples were not comparable and were ignored. Although there were 55 and 96 reads for K00174 and K00175, respectively, the numbers obtained for CAM were significantly lower than those for DBP (chi-square test; $p < 10^{-4}$). Occurrence of the two autotrophic reactions in ABP and MED was not likely, as there were <10 reads for these genes.

However, CO_2 can be fixed by other steps[23]. An enzyme encoded by K01595 (EC4.1.1.31) is able to fix CO_2 by using phosphoenolpyruvate, and another enzyme encoded by K00031 (EC1.1.1.42) consumes 2-oxoglutarate (also part of rTCA). In regions III and IV of Fig. 5, the two functional genes for CO_2 fixation were found in CAM and MED. K01595 was enriched in MED as previously reported[19], whereas K00031 was more abundant in CAM than in the other samples. Although not as abundant as in MED and CAM, K01595 and K00031 were also identified in DBP and were remarkably underrepresented in ABP.

KEGG and SEED annotations of cORFs for ABP and DBP were illustrated by MEGAN[21]. DBP possessed the Calvin-Benson-Bassham cycle (CBB) for CO_2 fixation. There were 19 cORFs for fructose 1.6-bisphosphatase type V (archaeal) and three for type I, whereas only four cORFs were discovered for ABP. Next, we compared some key enzymes in CO_2 fixation via the rTCA and rACA pathways. EC1.2.7.3 and EC1.2.7.1 displayed 228 cORFs in DBP, in contrast to six cORFs in ABP. In addition, EC1.1.1.42 and EC4.1.1.31 had 131 cORFs in DBP; a total of 52 such cORFs were identified in ABP. Fixation via these ECs in DBP was supported by abundant cORFs responsible for the supply of acetyl-CoA and phosphoenolpyruvate, which were six to nine-fold more abundant in DBP than in ABP.

Taxonomic assignment of the cORFs for four KEGG genes in DBP is illustrated in Figure 6. These were the most abundant genes in individual steps of autotrophic and anaplerotic CO_2 fixation. A total of 66 K00174 cORFs were derived mainly from Archaea and were occupied nearly 50% by the homologs of *Thermofilum* (Crenarchaeota). Ninety-three K00031 cORFs were evenly

distributed across several genera. Two of them, *Salinibacter* and *Meiothermus*, belonged to the bacteria, and the majority of the remainders were Halobacteriales in the Euryarchaeota. The 38 K01595 cORFs were highly represented by those cORFs from *Meiothermus*, and the 81 K00169 cORFs were largely occupied by *Halorhabdus* and some methanogens. In ABP, six K00174 cORFs showed a high level of similarity to the homologs from *Bradyrhizobium*. There were 13 K01595 cORFs, likely belonging to *Cupriavidus*. The 39 K00031 cORFs were probably associated with *Aromatoleum* and *Cupriavidus*.

Anaerobic methane oxidation by Archaea. Because methane dominates the gas mixtures released into ABP and DBP, microbes involved in AOM might play an important role in autotrophy. At present, three AOM archaeal groups (ANME1, ANME2, and ANME3) have been identified: ANME2 and ANME3 belong to the order Methanosarcinales, whereas ANME1 is more distantly related[24]. The functional gene *mcrA* (Methyl Coenzyme M Reductase A) was the target in studies of AOM and methanogens. In the metagenomes, a BLAST search facilitated the identification of a few *mcrA* reads only in DBP. Similarly, clones were successfully obtained from DBP but not from ABP.

Phylogeny of *mcrA* genes was reconstructed using proteins deduced from the cloned sequences and homologs. Although they were poorly supported by low bootstrap values, 17 *McrA* cloned protein sequences clustered with two ANME3 *McrA* proteins identified in the Cascadia margin sediment and in the Arctic sediment[25,26] (Fig. 7). Together, they were distant from the other ANME3 *McrA* proteins. Only one cloned sequence (no. 65) grouped with a known ANME3 *McrA* protein from *Methanohalophilus*. These two proteins were much closer to the main branch of ANME3 than those in the 17 cloned sequences. *McrA* proteins belonging to ANME1 and other cloned sequences were separated from the other clades. The protein sequence from clone no. 43 grouped with the ANME1 *McrA* sequences; the other 14 *McrA* sequences from the clones formed an independent internal clade that was distantly related to the ANME1 group. The large dissimilarity of some DBP *McrA* proteins compared with others confers their unique status among all known *mcrA* genes and supports their identification as a potentially new ANME group.

Brine and deep-sea water sample-specific COG pathways. With statistical analyses, COG pathways showing a significant difference ($p < 0.05$) between ABP and DBP were obtained. The DBP metagenome had significantly more genes that participate in biosynthesis pathways, including amino acids, nucleotides, heme, CoA and NAD (Table S2). Active hydrocarbon metabolic processes in DBP were inferred from the presence of significantly enriched pathways involved in glycolysis, gluconeogenesis and carbohydrate transport. The ABP metagenome displayed significant differences in cell wall/membrane/envelope biogenesis, inorganic ion transport and metabolism, cell motility and transcriptional regulators. Other pathways, such as flagellum biogenesis and lipid A biosynthesis, were considered as supplementary to these four large pathways (Table S2).

There were likely pathways involved in the adaptation to deep-sea water or the hydrothermal brine environment. Considering differences in the gene profiles, they were expected to be commonly enriched in both metagenomes from deep-sea water or the brine environment. COG pathways in ABP and DBP were separately compared with those of the deep-sea water metagenomes, and commonly enriched pathways in ABP and DBP included the following: menaquinone and ubiquinone biosynthesis, the multi-subunit Na^+/H^+ antiporter, carbohydrate transport and metabolism, and transcription and transcriptional regulators. Conversely, CAM and MED were compared separately with the brine samples, and COG pathways that were commonly enriched in the deep-sea water metagenomes comprised the following: F_0F_1-type ATP synthase subunits, the glyoxylate circle, Na^+-transport via NADH:ubiquinone oxidoreductase subunits, the TCA cycle, and protein translation, location and modification. The deep-sea samples also featured a variety of biosynthetic activities such as biosynthesis of amino acids, biotin, coenzyme A, heme, terpenoid, and the cell wall/membrane/envelope.

Some of these COG pathways are illustrated in Figure 5. However, novel findings were also obtained. The glyoxylate cycle is a shortcut pathway in the TCA cycle, and succinate is produced through the use of isocitrate in the shortcut[27]. Consequently, two CO_2 fixation steps in the reductive TCA cycle are bypassed. The strong activity of the glyoxylate cycle in deep-sea water samples was coincident with a low abundance of bypassed genes in the TCA cycle. There was a remarkable enrichment of isocitrate lyase (COG2224) and malate synthase (COG2225) genes in CAM and MED compared to ABP and DBP. Chi-square tests were conducted to compare the two COGs between the brine pool metagenomes and deep-sea water counterparts. Excluding the comparison of COG2224 between ABP and CAM, all of the other comparisons showed a significant difference

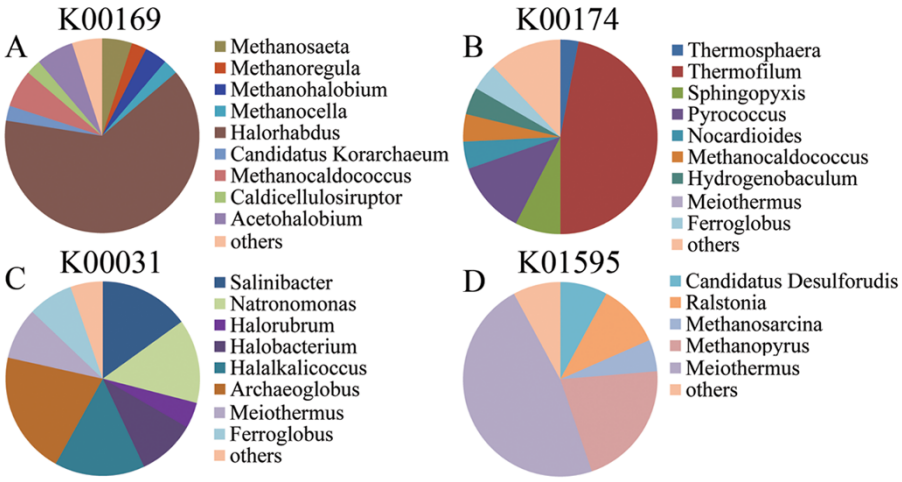

Figure 6 | Taxonomic assignment of CO_2 fixation genes in DBP. The KEGG genes, K00169 (A), K00174 (B), K00031 (C) and K01595 (D) were represented by complete ORFs extracted from reads of DBP. The genera of four functional KEGG genes involved in CO_2 fixation were summarized from the best hits obtained in the BLAST results against the NCBI-nr database (E-value $<10^{-4}$, score >60). Excluding *Methanosaeta*, the average of the BLAST scores for individual genera exceeded 100.

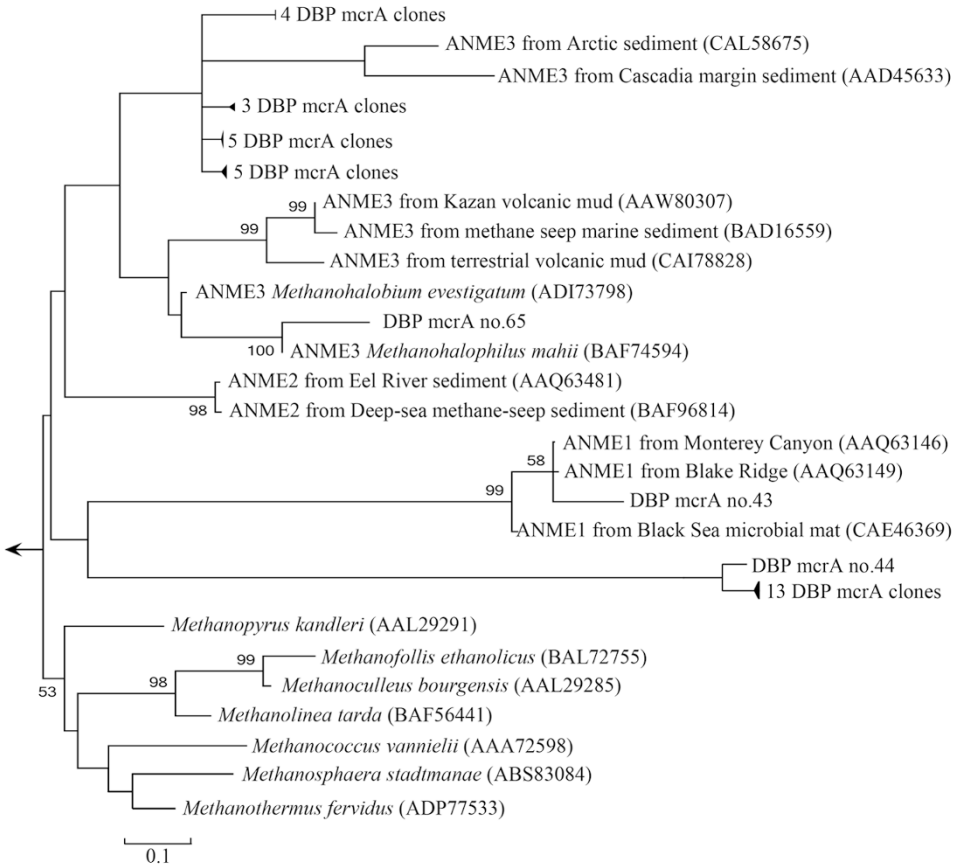

Figure 7 | Phylogeny of *McrA* partial sequences. The rooted maximum likelihood tree was reconstructed using known *McrA* partial sequences and translated amino acids from *mcrA* gene cloning sequences. Species names (or sampling site) and amino acid accessions of the sequences are shown. Bootstrap values were based on 1000 replicates; only those with a value > 50% are shown.

(chi-square test; $p < 10^{-4}$). In addition, different types of sodium pumps were detected. In the brine samples, a multi-subunit Na^+/H^+ antiporter was strongly represented by the corresponding gene, whereas in the deep-sea water samples, Na^+-transportation coupled with complex I in oxidative phosphorylation was utilized as a transport pathway[28,29]. Between the brine metagenomes, both Na^+ transport systems were significantly more abundant in DBP (Table S2).

Discussion

In the present study, brine pool metagenomes in the Red Sea were analyzed and compared with deep-sea water metagenomes. The results revealed drastic differences in the composition of the communities and metabolic spectra between the brine pool metagenomes. Although the two metagenomes have been compared in our previous work, only aromatic-degrading bacteria and metabolic pathways were examined to document the presence of aromatic compounds in the Atlantis II brine pool[15]. The current study elaborates on how the two brine pool ecosystems can be further differentiated via a comprehensive comparison of the microbial communities and their potential functions. In particular, we revealed archaeal taxa and metabolic pathways that have not been previously observed[15]. The samples from adjacent brine pools revealed that our two brine metagenomes differed even more remarkably than the deep-sea reference metagenomes sampled at widely separate sites and could not be grouped due to their high level of dissimilarity. Considering the historical connection of the two brine pools[8], the ecosystem in the Discovery brine pool might have been similar to that in the Atlantis II in the past. The present physical separation likely resulted in decrease in volume of the two brine pools, which has been reported in previous studies[9]. After the separation of the two brine pools, the exposure of Atlantis II to increasingly strong geothermal activities on the sea floor probably changed the original environment of Atlantis II. For example, in ABP, we did not find methanogens, AOM Archaea or other autotrophic microbes, which were present in DBP. The apparent absence of chemoautotrophic microbes in ABP might have completely converted the mode of life in this pool to heterotrophy. The present study provides evidence that microbes in ABP depended heavily on extracellular organic carbon, including aromatic compounds, non-aromatic heterocyclic compounds, amino acids, storage sugars and structural sugars in the surrounding water. Overall, conditions in the present lower convective layer of Atlantis II brine pool have selected against archaeal autotrophic and methanogenic inhabitants, while imposed minor effects on the bacterial residents. However, the elimination of these autotrophic inhabitants was probably not as extreme as demonstrated in this study. Considering the low cell density in the ABP sample, sampling drift and the experimental approach could have influenced our results. Crenarchaeotic marine group I (1.7%), Methanomicrobia (0.07%), Halobacteria (0.08%) and Archaeoglobi (0.15%) were detected in the lower convective layer of Atlantis II in an independent study (unpublished data). However, diversified archaeal groups were detected in the subsuperficial sediments of ABP by Siam et al. (2012)[30]; however, their proportion in the whole community was not determined. In the same report, Archaea were also identified in DBP sediment samples, whereas Crenarchaeota dominated the archaeal communities rather than Euryarchaeota, which consisted of the overwhelming majority of Archaea in the overlying brine in the present study. The differences between the two studies may be a consequence of environmental changes in the sediments. Although more Archaea can probably be

identified in Atlantis II, it is clear that the archaeal community in that pool has drastically diminished relative to that in the Discovery brine pool, potentially to the edge of extinction.

A considerable fraction of the archaeal community in DBP was believed to be capable of fixing CO_2, but these representatives were almost absent from ABP. This difference might be explained by CO_2 limitations in ABP. Although *in situ* CO_2 concentration in the Atlantis II brine pool was not measured, a body of evidence from the following geochemical analyses of brine water and sediments has suggested a very low CO_2 concentration in Atlantis II. In several sediment cores, manganosiderite minerals were much more abundant in Atlantis II than in all of the other brine pool sediments in the Red Sea[1]. These minerals were formed by the interaction of Fe^{2+} and Mn^{2+} ions with CO_2. The sources of CO_2 could be the hydrothermal fluids and biogenic $CaCO_3$ that dissolved in the brines at low pH values[1]. However, in such a scenario, almost all the CO_2 would be accepted rapidly by Mn and Fe ions that are injected into the brine pool via geochemical activities. Concentrations of Mn and Fe ions in the lower convective layer of the Atlantis II brine pool were much higher (Fe, 120×; Mn, 28×) than those in Discovery (Ref. 1 and our unpublished data). CO_2 in the lower layer of the Atlantis II could be easily fixed by the large amount of Mn and Fe ions and precipitated as manganosiderite in the sediments. Therefore, deprivation of CO_2 by metal ions limited CO_2-dependent autotrophy, particularly for the archaeal groups as indicated in the present study. In contrast, CO_2 fixation might also be conducted by bacteria such as *Cupriavidus*, *Salinibacter* and *Meiothermus*; however, the latter two genera were not found in ABP, perhaps because the extreme environment of the Atlantis II pool inhibited their colonization. This finding might also partially explained by the compositional differences in the bacterial communities between brine metagenomes at the phylum level because *Meiothermus* and *Salinibacter* represent Deinococcus-Thermus and Bacteroidetes/Chlorobigroup, respectively. Hence, the CO_2 limitation in Atlantis II likely also accounted for the elimination of CO_2 autotrophic Archaea and some bacterial inhabitants. Regarding *Cupriavidus* spp. in ABP, the question is whether the involved genes were present to fix CO_2 or to function in the reverse direction. These genes play a role in several different metabolic pathways. It is also a possibility that the genes were not expressed under low CO_2 concentrations. Furthermore, *Cupriavidus* can degrade aromatic compounds[31], and thus, their life mode might be heterotrophic in Atlantis II where organic maturation continues to occur[15]. The major role of *Cupriavidus* in Atlantis II was probably metal precipitation, as it is well known that *Cupriavidus* spp. are capable of precipitating different metal ions[32,33].

CO_2 fixation was also reported in a recent metagenomic study examining a Mediterranean deep-sea brine lake (DHAL)[34]. DBP and DHAL brine samples shared some taxonomic microbial assemblages such as Firmicutes and Gammaproteobacteria. Moreover, almost all types (CBB, cTCA and cACA) of CO_2 fixation uncovered in this study were performed by Euryarchaeota and Gammaproteobacteria present in the DHAL brine sample (a phosphoenolpyruvate-related type of CO_2 fixation was not described)[34]. However, the presence of CO_2 autotrophic Crenarchaeota in DBP is an important difference between these two deep-sea brine pools.

High concentrations of methane derived from hydrothermal fluids have been reported for the Atlantis II pool[13,35]. In such an environment, methane is normally consumed by AOM from the ANME3 group, which uses manganese oxide as an oxygen donor[36]. Because Discovery pool may be less disturbed by hydrothermal fluids, manganese oxides could be maintained at the sub-floor and likely be supplied by those manganese oxides generated in Atlantis II that spread into Discovery via deep-sea water circulation around the Chain brine pool (refer to the deep-sea water channel in Fig. 1). As a result, the lower convective layer of Discovery could support the rapid assimilation of methane by ANME3, thus explaining the presence of ANME3 methanotrophic Archaea in DBP. The case differs in Atlantis II, where manganese ions are still oxidized at the interface between the deep-sea water and the brine pool[1]. Manganese oxides then transfer the oxygen to ferrous ions in the upper convective layer, especially at the boundary between the lower and upper brine layers of the brine pool[1], resulting in the large-scale precipitation of ferrous oxides rather than manganese oxides to the sub-floor. There is evidence that Mn-hydroxides do not accumulate at the bottom of this pool as they do in Discovery, but rather, they have fallen to the slopes around the interface along the periphery of the Atlantis II brine pool and even in Discovery[1]. Hence, methane oxidation by ANME3 might occur at the interface of the Atlantis II pool and the seawater. As expected, *mcrA* sequences identical to those of ANME3 in DBP had been successfully cloned using the water sample collected from the interface of Atlantis II (unpublished data). Although Fe hydroxide also can be potentially used for methane oxidation by ANME3, Mn hydroxide is preferred due to its five-fold higher potential for free energy gain[36]. Therefore, the interface between the Atlantis II brine pool and the deep-sea water was found to be a better niche for ANME3. In addition, a novel branch was identified in our phylogenetic tree. Because no *mcrA* cloning sequences clustered with the known methanogens, they were likely derived from methanogenic Archaea. Without additional evidence, however, their role in ABP remains unclear.

However, methane can be consumed by methanotrophic microbes that possess monooxygenase (encoded by the *pmo* and *mmo* genes)[37]. We used monooxygenase proteins to search for possible homologs in the four metagenomes. Positive results (BLAST cutoff score of 100) were obtained only for the CAM metagenome, in which uncultured crenarchaeota and methanotrophic bacteria (Methylococcaceae) were candidates for the consumption of methane under aerobic conditions. A high expression level of *pmo* genes was confirmed in a recent metatranscriptomic study of a seawater sample from the Carmen Basin, Gulf of California[20].

The presence of aromatic compounds in the lower convective layer of Atlantis II has been reported in our previous work[15]. In theory, the increasing temperature in the Atlantis II brine pool has converted organic carbons into aromatic compounds[15]. The change in carbon sources under high temperatures can affect microbial communities and metabolic activities dramatically. Aromatic compounds have seldom been reported as carbon sources for Archaea. For methanogens, alkanes, acetate and volatile fatty acids are typically used to produce methane[38–40]. If the methanogens were the original inhabitants of Atlantis II, sufficient labile carbon was not easy to access in the lower convective layer. Therefore, the exclusion of archaeal methanogens is likely ascribed to the conversion of organic carbon into aromatic compounds. This would also have limited the diversity of the bacterial communities because only those capable of degrading aromatic compounds could proliferate in the lower convective layer of Atlantis II.

We have argued that carbon sources contributed to the compositional shift in ABP. Environmental stresses imposed by chemocline, thermocline, halocline and heavy metal content could have greatly impacted the microbes. To cope with chemocline and thermocline, microbes may employ chemotactic mechanisms to sense surrounding environmental changes; Bacteria and Archaea can react to changes in chemical factors by switching their motility, speed and the direction of their flagella[41]. ABP possessed a greater number of chemotactic genes; for example, it had four times more *mcp* (methyl-accepting chemotaxis protein) genes compared with DBP. More detailed comparisons between ABP and DBP with respect to chemotactic genes and pathways have been reported in our previous work[15]. Surprisingly, in the current study, related pathways for flagellar assembly and bacterial chemotaxis demonstrated greater enrichment in MED than in all of the other metagenomes evaluated. The significant enrichment for the chemotaxis in MED was considered to be an

adaptation to the extreme lack of nutrients in Mediterranean deep-sea water (Ref. 19 and references therein). One may argue that the pursuit of nutrients is even more important than the stresses imposed by chemocline and thermocline in the lower convective layer of the Atlantis II pool. Perhaps, the enrichment of chemotactic genes in ABP relative to DBP was also due to a shortage in the nutrient supply.

Two approaches, via the NADH:ubiquinone Na^+ antiporter and the multi-subunit Na^+/H^+ antiporter, were discovered in the four metagenomes. First, multi-subunit Na^+/H^+ antiporter genes were significantly enriched in both of the brine metagenomes. Because the salinity of the sampling sites in the brine pools was much higher than that in the deep-sea waters (34.6‰ for CAM and 38.7‰ for MED), the multi-subunit Na^+/H^+ antiporter approach likely played a more important role in microbial adaptation to extreme salinity. Second, the comparison between the two brine metagenomes revealed that both antiporters were more strongly represented by the reads in DBP. Despite the same salinity at the two sites, this result suggested that microbes in DBP, surprisingly, possessed more Na^+ transporter genes than did those in ABP. The NADH:ubiquinone Na^+ antiporter is the dedicated Na^+ pump in many aerobic bacteria[42]. As expected, this pump was significantly enriched in the deep-sea water metagenomes in the present study, as compared with ABP and DBP. The pumping process is supposed to be coupled to the strong oxidative phosphorylation that occurs in deep-sea water metagenomes and, therefore, to serve as an adaptive strategy in oxic seawater environments. Furthermore, a large number of ATPs generated by the oxidative phosphorylation process could drive various biosynthetic activities, thus explaining the enrichment of biosynthesis genes in deep-sea water metagenomes.

Considering the ongoing strong metal precipitation activities[1], the Atlantis II brine pool imposes a stronger impact on microbial inhabitants that are exposed to a large amount of metal ions and a higher temperature, compared with those present in the Discovery. However, in DBP, we identified more metal ion pumps for cobalt, nickel, manganese and iron, which suggests that these metal transport processes are important for the microbes in DBP. In addition, there was a lack of a correspondingly high abundance of metal transporter genes in ABP, although manganese and iron were the major types of metal ions present in the lower convective layer of Atlantis II[1]. The microbes in ABP elected energy-saving mechanisms, likely because these pumps are energy-dependent ABC transporters. This phenomenon was exemplified by a two-component copper transport system encoded by the *cus* operon that had significantly more genes in ABP than in DBP.

Most of the adaptive mechanisms discussed above may explain the adaption observed for the microbes in DBP. However, the mechanism by which microbes adapted to the complex and extreme conditions in the Atlantis II brine pool remains unclear. To address this issue, the enriched pathways in ABP were further examined, and their possible adaptive roles were explored. Transcriptional regulators were clearly important for a rapid response to the fluctuation of variant factors in the Atlantis II brine pool. The enrichment of genes for secretion systems IV and VI in ABP also suggested a potentially important mechanism. Six types of secretion systems have been identified thus far[43]. The secretion system IV has been recently reported in thermophilic bacteria and is thought to govern the transfer of DNA and protein between cells[44].

Because our conclusions are based on analyses of metagenomes from a small volume of brine water, further transcriptomic studies are required to support our findings regarding autotrophic metabolism. A comprehensive survey of microbial communities should be undertaken at more sampling sites with replicates to determine whether the microbial communities changed dramatically in the different layers and at different sites in the same layers of the brine pools.

Methods

Sampling. Water samples were collected from the Atlantis II and Discovery brine pools during an R/V OCEANUS cruise in October 2008[16]. Both samples were obtained from the lower convective layers of the pools (>2100 m). At each sampling site, 4 L of brine water was immediately filtered through a 1.6 μm GF/A membrane (diameter 125 mm; Whatman, Clifton, NJ) followed by a 0.22 μm Steripak-GP polyethersulfone membrane (Millipore, Bedford, MA) to capture prokaryotic cells. Total genomic DNA was extracted and purified according to the SDS-based method described by Huber et al. (2002)[45]. Temperature, depth, and salinity were recorded by a CTD unit.

Microbial cell counting. Three replicates of each 10-mL sample were immediately fixed with formaldehyde. The fixed samples were then filtered through polycarbonate membranes (0.2 μm, 25 mm diam., Isopore; Millipore, Bedford, MA) and stained with 4,6-diamidino-2-phenylindole (DAPI) for 15 min in the dark. Cells were counted in 10 randomly selected fields using an Olympus epifluorescence microscope (FSX100, Hamburg, Germany).

Metagenome analyses. Pyrosequencing of the two brine pool metagenomes was performed as described previously[15]. Because no deep-sea brine metagenomes were available in the public databases, two reference deep-sea water metagenomes were obtained from the CAMERA (camera.calit2.net) and NCBI-SRA (www.ncbi.nlm.nih.gov/sra) databases. CAM (accession ID: CAM_S_465 in CAMERA) was sampled near a deep-sea hydrothermal vent in Carmen Basin, Gulf of California (26°38′N, 110°72.8′W). The depth, temperature and salinity of the sampling site were 1900 m, 2.6°C and 34.6‰, respectively. MED is referred to as SRX087122 in the NCBI-SRA. MED was sampled at 4,908 m in the Matapan-Vavylov Deep, Mediterranean Sea at (36°34.00'N, 21°07.44'E)[19]. The temperature and salinity were 14.3°C and 38.7‰, respectively. Because the microbial community in MED was relatively simple[19], only a small portion of the MED metagenome (557,800 reads) was used in the present study. The reads were randomly selected from the original file.

16S rRNA gene fragments in the reads were identified using Meta-RNA[46] and extracted with an in-house program. Using cdhit-454[47], duplications that occupied 20–30% of the fragments were removed, and the longest representatives among the duplicates were retained. Taxonomic classification of the fragments was conducted with the RDP naïve Bayesian Classifier version 2.5 (http://rdp.cme.msu.edu/). A confidence threshold of 50% was applied to the classification at phylum and genus levels[48]. Because *Ralstonia* and *Wautersia* have been jointly combined with *Cupriavidus*[49], the percentage of *Cupriavidus* was the total percentage of the three genera. The protocol used herein contained several modifications compared with that introduced in our previous work[15], but the percentage of dominant bacterial genera such as *Cupriavidus* remained almost the same.

Pyrosequencing reads were used to BLAST against the two protein databases, KEGG (version 51)[50] and COG (http://string-db.org), using an e-value of $<10^{-4}$. The results of the BLAST search were summarized by selecting the best hits as KEGG genes or COGs in the reads. EC numbers were also extracted from the KEGG gene annotation. Redundant reads from pyrosequencing emPCR amplification and whole genome amplification were filtered using an in-house tool. The algorithm employed for the redundancy clearance was as follows: reads for the same KEGG genes and COGs were aligned pairwise and evaluated for identical portions (in a size of 50 bp) on both strands. The identical portions did not occur exactly at the first position of the two reads and could be shifted slightly. Shorter reads were removed if they contained portions identical to those in one of the longer reads.

The numbers of KEGG genes, COGs and ECs were standardized separately. A Bray-Curtis dissimilarity matrix was calculated from each of the three datasets. AHC analysis was performed using the pvclust package in the R project. Ward's method was employed for agglomerative hierarchical clustering. In addition, the dissimilarity matrix was used in the PCoA analysis.

The KEGG dataset was then normalized using a z-score, and the genes were clustered using Cluster3[51]. A complete linkage method and a metric of correlation (uncentered) were employed during the clustering of samples and genes. The KEGG genes in the five sample-specific gene clusters shown in Figure 5 were sorted into different KEGG pathways. In Figure 5, only pathways with more than 10 genes or those with at least 50% of all the genes in a given pathway are displayed. However, some pathways contained genes that were shared with some of the other pathways. To avoid over counting such genes, at least two pathway-specific genes were identified in a selected pathway. The positions of the genes in the KEGG pathway maps were rechecked to confirm their involvement in the essential function of a given pathway. Sorting of the genes into KEGG functional modules was performed using the same approach. In the modules selected for comparison, at least 50% of their KEGG genes had been identified in the metagenomes.

We did not conduct homopolymer error correction for the four metagenomes. For the brine pool metagenomes, the cORFs were extracted from reads longer than 200 bp and defined as those covering whole reads without interruptions except for the last five positions. This strategy may preclude the use of reads with a premature termination of the ORF, which often occurs in pseudogenes or reads with a low pyrosequencing quality. A BLAST search was performed against the NCBI protein database, and the taxonomies for the resultant hits (score >60) were summarized using MEGAN[21]. The KEGG and SEED genes assigned to different pathways could also be visualized through the use of MEGAN. Using ShotgunFunctionalizeR in the R project, the COGs in the cORFs were compared to identify genes and pathways that differed significantly in relative abundance. P-values were adjusted using the Bonferroni correction.

Phylogeny reconstruction using cloned *mcrA* genes from DBP. Forward and reverse primers used for PCR amplification of *mcrA* genes were 5′-TAYGAYCARATHTGGYT-3′ and 5′-ACRTTCATNGCRTARTT-3′, respectively[52]. Each cycle (total of 30 cycles) consisted of a 60 s denaturation step at 94°C, a 45 s annealing step at 45°C, and a 50 s elongation step at 72°C. Each PCR reaction (total of 25 μl) contained 2.5 μL of 10XPCR buffer, 2 μL of 2 mM dNTP, and 1 U of Taq DNA Polymerase (Takara, Tokyo, JP). The PCR products were purified and cloned using the TOPO-TA Cloning Kit (Invitrogen, Carlsbad, CA, USA) according to the manufacturer's protocol. The sequences were deposited in NCBI (accession numbers: JX907770-JX907800). Next, the translated proteins were aligned with other *McrA* protein sequences collected from NCBI using MUSCLE3.5[53] . The alignment was manually checked to remove gaps and was then used to reconstruct a neighbor-joining (NJ) tree with 1000 bootstrap replicates using MEGA5[54]. A maximum likelihood (ML) phylogenetic tree with 1000 bootstrap replicates was then built, using the NJ tree as an internal tree. Jones_Taylor_Thornton was selected as the substitution model. *McrA* sequences from methanogens served as the outgroup for the rooted ML tree.

1. Gurvich, E. G. In *Metalliferous Sediments of the World Ocean* (Springer Berlin Heidelberg, 2006).
2. Ramboz, C., Oudin, E. & Thisse, Y. Geyser-type discharge in Atlantis II Deep, Red Sea: evidence of boiling from fluid inclusions in epigenetic anhydrite. *Can Mineral* **26**, 765–786 (1988).
3. Oudin, E., Thisse, Y. & Ramboz, C. Fluid inclusion and mineralogical evidence for high temperature saline hydrothermal circulation in the Red Sea metalliferous sediments: preliminary results. *Mar. Mining* **5**, 3–31 (1984).
4. Miller, A. R. *et al*. Hot brines and recent iron deposits in deeps of the Red Sea. *Geochim Cosmochim Acta* **30**, 341–350 (1966).
5. Girdler, R. W. A review of Red Sea heat flow. *Phil Trans Roy Soc Lon A* **267**, 191–203 (1970).
6. Schoell, M. & Hartmann, M. Detailed temperature structure of the hot brines in the Atlantis II Deep area (Red Sea). *Marine Geol* **14**, 1–14 (1973).
7. Blanc, G. & Anschutz, P. New stratification in the hydrothermal brine system of the Atlantis II Deep, Red Sea. *Geology* **23**, 543–546 (1995).
8. Turner, J. S. *A physical interpretation of the observations of hot brine layers in the Red Sea.* (Springer, Berlin; 1969).
9. Monnin, C. & Ramboz, C. The anhydrite saturation index of the ponded brines and sediment pore waters of the Red Sea deeps. *Chem Geol* **127**, 141–159 (1996).
10. Ross, D. A. & Hunt, J. M. Third brine pool in the red sea. *Nature* **213**, 687–688 (1967).
11. Swallow, J. C. & Crease, J. Hot salty water at the bottom of the Red Sea. *Nature* **205**, 165–166 (1965).
12. Hartmann, M., Scholten, J. C., Stoffers, P. & Wehner, F. Hydrographic structure of brine-filled deeps in the Red Sea--new results from the Shaban, Kebrit, Atlantis II, and Discovery Deep. *Marine Geology* **144**, 311–330 (1998).
13. Faber, E. *et al*. Methane in Red Sea brines. *Organic Geochem* **29**, 363–379 (1998).
14. Anschutz, P. & Blanc, G. Heat and salt fluxes in the Atlantis II Deep (Red Sea). *Earth Planet Sci Lett* **142**, 147–159 (1996).
15. Wang, Y. *et al*. Hydrothermally generated aromatic compounds are consumed by bacteria colonizing in Atlantis II Deep of the Red Sea. *ISME J* **5**, 1652–1659 (2011).
16. Swift, S. A., Bower, A. S. & Schmitt, R. W. Vertical, horizontal, and temporal changes in temperature in the Atlantis II and Discovery hot brine pools, Red Sea. *Deep Sea Res I* **64**, 118–128 (2012).
17. Cole, J. R. *et al*. The Ribosomal Database Project: improved alignments and new tools for rRNA analysis. *Nucl. Acids Res.* **37**, 141–145 (2009).
18. Dick, G. J. & Tebo, B. M. Microbial diversity and biogeochemistry of the Guaymas Basin deep-sea hydrothermal plume. *Environ Microbiol* **12**, 1334–1347 (2010).
19. Smedile, F. *et al.* Metagenomic analysis of hadopelagic microbial assemblages thriving at the deepest part of Mediterranean Sea, Matapan-Vavilov Deep. *Environ Microbiol* **15**, 167–182 (2012).
20. Lesniewski, R. A., Jain, S., Anantharaman, K., Schloss, P. D. & Dick, G. J. The metatranscriptome of a deep-sea hydrothermal plume is dominated by water column methanotrophs and lithotrophs. *ISME J* **6**, 2257–2268 (2012).
21. Huson, D. H., Mitra, S., Ruscheweyh, H.-J., Weber, N. & Schuster, S. C. Integrative analysis of environmental sequences using MEGAN4. *Genome Res* **21**, 1552–1560 (2011).
22. Pitcher, R. S. & Watmough, N. J. The bacterial cytochrome cbb3 oxidases. *Biochim. Biophys. Acta* **1655**, 388–399 (2004).
23. Hügler, M., Huber, H., Stetter, K. O. & Fuchs, G. Autotrophic CO_2 fixation pathways in archaea (Crenarchaeota). *Arch Microbiol.* **179**, 160–173 (2003).
24. Knittel, K. & Boetius, A. Anaerobic oxidation of methane: progress with an unknown process. *Ann Rev Microbiol* **63**, 311–334 (2009).
25. Hallam, S. J., Girguis, P. R., Preston, C. M., Richardson, P. M. & DeLong, E. F. Identification of methyl coenzyme M reductase A (mcrA) genes associated with methane-oxidizing archaea. *Appl Environ Microbiol* **69**, 5483–5491 (2003).
26. Losekann, T. *et al.* Diversity and abundance of aerobic and anaerobic methane oxidizers at the Haakon Mosby mud volcano, Barents Sea. *Appl Environ Microbiol* **73**, 3348–3362 (2007).
27. Kornberg, H. L. The role and control of the glyoxylate cycle in Escherichia coli. *Biochem J.* **99**, 1–11 (1966).
28. West, I. C. & Mitchell, P. Proton/sodium ion transport in Escherichia coli. *Biochem. J* **144**, 87–90 (1974).
29. Stolpe, S. & Friedrich, T. The Escherichia coli NADH:Ubiquinone oxidoreductase (complex I) is a primary proton pump but may be capable of secondary sodium antiport. *J Biol Chem* **279**, 18377–18383 (2004).
30. Siam, R. *et al.* Unique prokaryotic consortia in geochemically distinct sediments from Red Sea Atlantis II and Discovery Deep brine pools. *PLoS ONE* **7**, e42872 (2012).
31. Pérez-Pantoja, D., De la Iglesia, R., Pieper, D. H. & González, B. Metabolic reconstruction of aromatic compounds degradation from the genome of the amazing pollutant-degrading bacterium Cupriavidus necator JMP134. *FEMS Microbiol Rev.* **32**, 736–794 (2008).
32. Lykidis, A. *et al.* The complete multipartite genome sequence of Cupriavidus necator JMP134, a versatile pollutant degrader. *PLoS ONE* **5**, e9729 (2010).
33. Reith, F. *et al.* Mechanisms of gold biomineralization in the bacterium Cupriavidus metallidurans. *Proc Natl Acad Sci USA* **106**, 17757–17762 (2009).
34. Ferrer, M. *et al.* Unveiling microbial life in the new deep-sea hypersaline Lake Thetis. Part II: a metagenomic study. *Environ Microbiol* **14**, 268–281 (2011).
35. Schmidt, M. *et al.* High-resolution methane profiles across anoxic brine-seawater boundaries in the Atlantis-II, Discovery, and Kebrit Deeps (Red Sea). *Chem Geol* **200**, 359–375 (2003).
36. Beal, E. J., House, C. H. & Orphan, V. J. Manganese- and iron-dependent marine methane oxidation. *Science* **325**, 184–187 (2009).
37. Lipscomb, J. D. Biochemistry of the soluble methane monooxygenase. *Ann Rev Microbiol* **48**, 371–399 (1994).
38. Zengler, K., Richnow, H. H., Rossello-Mora, R., Michaelis, W. & Widdel, F. Methane formation from long-chain alkanes by anaerobic microorganisms. *Nature* **401**, 266–269 (1999).
39. Sorensen, J., Christensen, D. & Jorgensen, B. B. Volatile fatty acids and hydrogen as substrates for sulfate-reducing bacteria in anaerobic marine sediment. *Appl. Environ. Microbiol.* **42**, 5–11 (1981).
40. Zinder, S. H. In *Methanogenesis: ecology, physiology, biochemistry and genetics.* (ed. J. G. Ferry) (Chapman and Hall, New York; 1993).
41. Lux, R. & Shi, W. Chemotaxis-guided movements in bacteria. *Critical Rev Oral Biol Med* **15**, 207–220 (2004).
42. Hase, C. C., Fedorova, N. D., Galperin, M. Y. & Dibrov, P. A. Sodium ion cycle in bacterial pathogens: evidence from cross-genome comparisons. *Microbiol Mol Biol Rev* **65**, 353–370 (2001).
43. Economou, A. *et al.* Secretion by numbers: protein traffic in prokaryotes. *Mol Microbiol* **62**, 308–319 (2006).
44. César, C. E. *et al.* Unconventional lateral gene transferin extreme thermophilic bacteria. *Int Microbiol* **14**, 187–199 (2011).
45. Huber, J. A., Butterfield, D. A. & Baross, J. A. Temporal changes in archaeal diversity and chemistry in a mid-ocean ridge subseafloor habitat. *Appl. Environ. Microbiol.* **68**, 1585–1594 (2002).
46. Huang, Y., Gilna, P. & Li, W. Identification of ribosomal RNA genes in metagenomic fragments. *Bioinformatics* **25**, 1338–1340 (2009).
47. Niu, B., Fu, L., Sun, S. & Li, W. Artificial and natural duplicates in pyrosequencing reads of metagenomic data. *BMC Bioinformatics* **11**, 187 (2010).
48. Claesson, M. J. *et al.* Comparative analysis of pyrosequencing and a phylogenetic microarray for exploring microbial community structures in the human distal intestine. *PLoS ONE* **4**, e6669 (2009).
49. Vandamme, P. & Coenye, T. Taxonomy of the genus Cupriavidus: a tale of lost and found. *Int J Syst Evol Microbiol* **54**, 2285–2289 (2004).
50. Kanehisa, M. & Goto, S. KEGG: Kyoto Encyclopedia of Genes and Genomes. *Nucl Acids Res* **28**, 27–30 (2000).
51. Eisen, M. B., Spellman, P. T., Brown, P. O. & Botstein, D. Cluster analysis and display of genome-wide expression patterns. *Proc Natl Acad Sci USA* **95**, 14863–14868 (1998).
52. Kendall, M. M. *et al.* Diversity of archaea in marine sediments from Skan Bay, Alaska, including cultivated methanogens, and description of Methanogenium boonei sp. nov. *Appl Environ Microbiol* **73**, 407–414 (2007).
53. Edgar, R. C. MUSCLE: multiple sequence alignment with high accuracy and high throughput. *Nucl Acids Res* **32**, 1792–1797 (2004).
54. Tamura, K. *et al.* MEGA5: molecular evolutionary genetics analysis using maximum likelihood, evolutionary distance, and maximum parsimony methods. *Mol Biol Evol* **28**, 2731–2739 (2011).

Acknowledgements

The authors are grateful to Prof. Paul Harrison for his comments on the manuscript. This study was supported by the National Basic Research Program of China (973 Program, No. 2012CB417304) and an award (SA-C0040/UK-C0016) granted to P.Y. Qian from the King Abdullah University of Science and Technology.

Author contribution

Y.W., O.O.L. and P.Y.Q. wrote the main manuscript. H.L.C., A.A.S. and G.S.Z. performed the experiments. Y.W. and H.L.C. analyzed the data. Y.W., O.O.L., S.B., A.A.S. and P.Y.Q. designed and prepared the samples. All authors discussed and reviewed the manuscript.

Additional information

Supplementary information accompanies this paper at http://www.nature.com/scientificreports

Competing financial interests: The authors declare no competing financial interests.

How to cite this article: Wang, Y. *et al.* Autotrophic Microbe Metagenomes and Metabolic Pathways Differentiate Adjacent Red Sea Brine Pools. *Sci. Rep.* **3**, 1748; DOI:10.1038/srep01748 (2013).